Frequency dependence of the Hall-potential distribution in quantum Hall systems: roles of edge channels and current contacts

Kousuke Shima and Hiroshi Akera

Division of Applied Physics, Faculty of Engineering, Hokkaido University, Sapporo, Hokkaido, 060-8628, Japan

Abstract

The spatial dependence of the Hall potential induced in a two-dimensional electron system (2DES) by AC source-drain voltage is studied theoretically in the incoherent linear transport in the strong-magnetic-field regime. The local capacitance approximation is employed, in which the potential at each point of the 2DES is proportional to the induced charge at the same point. It is shown that the frequency dependence of the induced charge distribution is described by three time constants, $\tau_{\rm e}$ for transport through an edge channel of the electron injected from a current contact, $\tau_{\rm eb}$ for transition between the edge channel and the bulk state, and $\tau_{\rm b}$ for diffusion into the bulk, which are quite different in magnitude: $\tau_{\rm e} \ll \tau_{\rm eb} \ll \tau_{\rm b}$ in the quantum Hall regime of a typical sample. These three time constants also determine how the Hall potential evolves in the 2DES after the source-drain voltage is turned on. Calculated two-dimensional distribution of the Hall potential as a function of the frequency reveals that the Hall potential develops by penetrating into the bulk from source and drain contacts as well as from the edge channel.

Keywords: quantum Hall effect, AC transport, current distribution, edge channel, edge magnetoplasmon

1. Introduction

A two-dimensional electron system (2DES) in a strong magnetic field, which is called a quantum Hall system, has a unique energy spectrum consisting of the Landau levels. This is the origin of various novel phenomena which have been observed in the quantum Hall system. The integer quantum Hall effect [1, 2] is caused by the energy gap between neighboring Landau levels and the localized states within the gap. The fractional quantum Hall effect [3] is due to the energy gap created when the electron correlation is brought into a single degenerate Landau level. Measurements on the AC transport through such a quantum Hall system have started soon after the discoveries of these quantum Hall effects to examine the influence of nonzero frequency on each of the quantum Hall effects [4, 5, 6]. However the AC response of such systems is not fully understood because it possesses a variety of features at different frequency scales. In this paper we propose a theoretical framework, for the AC transport through a quantum Hall system, which incorporates an edge channel originating from a Landau level and can treat low-frequency dynamics of the charge distribution associated with the edge channel and the bulk region.

Grodnensky et al. [7] have performed a contactless measurement on the response of a quantum Hall system to the AC electric field and observed a crossover from bulk to boundary response with increasing the angular frequency ω. They have also constructed [8] a diffusion equation for the induced potential, which is proportional to the induced charge in the local capacitance approximation, with a diffusion constant proportional to the local DC conductivity σ_{xx}^0 and derived a penetration length of the induced potential $\lambda(\omega) \propto (\sigma_{xx}^0/\omega)^{1/2}$, which explains the observed crossover. The same penetration length describes the Hall-potential distribution in the AC transport through a quantum Hall conductor, as has been shown later by one of the present authors [9]. The time constant τ for the response of the whole 2DES with size L is derived from $\lambda(\omega) = L$ and $\tau = \omega^{-1}$ and can be quite long when σ_{xx}^0 is vanishingly small in the quantum Hall regime. Such a slow dynamics in the quantum Hall system has actually been observed in several experiments [10, 11, 12, 13], and has also been incorporated in a theory on the breakdown of the quantum Hall effect [14].

The edge channel is formed in the presence of the confining potential which shifts a Landau level up to the Fermi level. The DC response of the edge channel is known to be remarkably different from that of the bulk region. In the steady state the nonequilibrium edge-channel population has been observed [15, 16, 17, 18, 19, 20, 21] in which the induced potential (more precisely the electrochemical potential) of the edge channel is largely deviated from that of the neighboring bulk region. This occurs because the electron transition between the edge channel and the bulk region is less frequent, resulting in a high effective resistance between the two regions. This high resistance is expected to give rise to another long time constant. The observation of the corresponding slow dynamics is anticipated.

The development of the potential in the edge channel is much faster than that in the bulk region and is initiated by the excitation of the edge magnetoplasmon. The edge magnetoplasmon has been studied experimentally [22, 23, 24, 25, 26] and theoretically [27, 28, 29, 30] in various 2DES's. The edge magnetoplasmon in some quantum Hall systems has been confirmed

Email address: akera@eng.hokudai.ac.jp ()

to be confined within the edge channel experimentally [31, 32] and theoretically [33]. The measured group velocity of the edge magnetoplasmon ranges from 10^4m/s to 10^7m/s depending on the filling factor and on whether a metallic gate is present in the vicinity of the edge channel or not [24, 32, 34, 35]. Then the time constant is from 10^{-7}s to 10^{-10}s for the full development of the potential in a 1mm edge channel.

Theories on the AC response of the quantum Hall system so far treated the response of the edge channel [1] and that of the bulk region separately as described above. A framework which can treat both responses in a unified manner is highly desirable. Such a framework is necessary, in particular, to clarify the AC response in the lower-frequency region where the bulk region starts to be excited in addition to the edge channel.

In this paper we develop a theoretical formulation (in Section 2) to describe the AC transport through a quantum Hall system taking into account responses of both the edge channel and the bulk region, each of which has a contact with the source and drain electrodes. In our model the time evolution is given by the equation of charge conservation in the local capacitance approximation. The current density which appears in this equation is given in terms of components of the local conductivity tensor, $\sigma_{xx}(\omega) = \sigma_{yy}(\omega)$ and $\sigma_{yx}(\omega) = -\sigma_{xy}(\omega)$, and a phenomenological conductance describing the electron transition between the edge channel and the bulk region. Using this model we first derive formulas of three time constants for the charge dynamics corresponding to the diffusion into the inside of the bulk region, the propagation along the edge channel, and the transition between the edge channel and the bulk region, respectively (in Section 3). Then we calculate one-dimensional distribution of the Hall potential along a cross-section perpendicular to the current (in Section 4) as well as two-dimensional distribution in the 2DES between current contacts (in Section 5) as a function of the angular frequency.

2. Formulation

2.1. Energy levels and conductivities of the 2DES

We consider a rectangular 2DES in the xy plane which is connected to source and drain electrodes at boundaries, $x = -L_x/2$ and $x = L_x/2$, respectively. In strong magnetic fields, the energy of an electron forms the Landau levels, which are broadened by the impurity potential. Due to the confining potential present outside of the bulk region ($|y| \le L_y/2$), each Landau level shifts toward the higher energy with increasing $|y|$. When such a level intersects with the Fermi energy outside of the bulk region, it forms an edge channel. A narrow region between the edge channel and the bulk region is called an incompressible region because the density of states at the Fermi energy is vanishingly small there. The level broadening by the impurity potential is less important in the presence of the confining potential which lifts the Landau-level degeneracy.

[1] The AC response of edge channels in a quantum Hall conductor with many terminals, such as current contacts and gate electrode, was studied theoretically and experimentally [41, 42].

The number of the edge channels increases with the Fermi energy. In this paper we consider only the system with a single edge channel. The corresponding Landau-level filling factor $\nu_{\rm b}$ in the bulk region with level broadening is in the range of $1 < \nu_{\rm b} < 3$ including the spin degeneracy. The local DC Hall conductivity σ^0_{yx} in the bulk has a quantized value of $2e^2/h$ in a range near $\nu_{\rm b} = 2$ due to the electron localization. Here we further restrict the range of $\nu_{\rm b}$ so that σ^0_{yx} has a quantized value of $2e^2/h$ in the bulk region.

We consider the incoherent transport, which is applicable except the region of very low temperatures. In the incoherent transport it is assumed that the current density $j_\alpha(\boldsymbol{r}, t) = j_\alpha(\boldsymbol{r}, \omega)e^{i\omega t}$ at the position $\boldsymbol{r} = (x, y)$ is determined only by the electric field at the same position $E_\beta(\boldsymbol{r}, t) = E_\beta(\boldsymbol{r}, \omega)e^{i\omega t}$ ($\alpha, \beta = x, y$):

$$j_\alpha(\boldsymbol{r}, \omega) = \sum_\beta \sigma_{\alpha\beta}(\boldsymbol{r}, \omega)E_\beta(\boldsymbol{r}, \omega). \tag{1}$$

The electric field is related to the gradient of the induced potential $\phi(\boldsymbol{r}, \omega)$ by $E_\beta(\boldsymbol{r}, \omega) = -\nabla_\beta\phi(\boldsymbol{r}, \omega)$. Although the current has another component produced by the gradient of the chemical-potential deviation $\Delta\mu$ from the equilibrium value, it is neglected in this paper because it has been shown in our previous paper [9] that $|\nabla_\beta\Delta\mu| \ll |e\nabla_\beta\phi|$.

In the above equation $\sigma_{\alpha\beta}(\boldsymbol{r}, \omega)$ is a component of the complex conductivity tensor. We assume that our 2DES is isotropic in the xy plane in equilibrium so that we have $\sigma_{xx}(\boldsymbol{r}, \omega) = \sigma_{yy}(\boldsymbol{r}, \omega)$ and $\sigma_{xy}(\boldsymbol{r}, \omega) = -\sigma_{yx}(\boldsymbol{r}, \omega)$. In addition we assume that our 2DES is uniform in equilibrium within the bulk region ($|x| \le L_x/2$ and $|y| \le L_y/2$) so that $\sigma_{\alpha\beta}(\boldsymbol{r}, \omega)$ in the bulk region has no dependence on the position and is denoted simply by $\sigma_{\alpha\beta}(\omega)$. In this paper we restrict our discussion to the low-frequency response, and therefore we retain terms up to the first order of ω in expansion of $\sigma_{\alpha\beta}(\omega)$ in a power series of ω. In our previous paper [9] we have obtained the following formulas of $\sigma_{xx}(\omega)$ and $\sigma_{xy}(\omega)$:

$$\sigma_{xx}(\omega) = \sigma^0_{xx} + i\omega\chi^0_{xx}, \quad \sigma_{xy}(\omega) = \sigma^0_{xy} \tag{2}$$

where σ^0_{xx} and σ^0_{xy} are the DC conductivities and χ^0_{xx} is the DC susceptibility. We use the values of the DC susceptibilities calculated in the absence of the impurity potential [9]: $\chi^0_{xx} = e^2\nu_{\rm b}/(h\omega_{\rm c})$ and $\chi^0_{xy} = 0$ where $\omega_{\rm c}$ is the cyclotron frequency. The DC Hall conductivity is $\sigma^0_{xy} = -2e^2/h$ as we have assumed before.

The electron transition between the edge channel and the bulk state at one of boundaries ($y_+ \equiv L_y/2$ and $y_- \equiv -L_y/2$) gives the current which cannot be described by the local conductivity $\sigma_{\alpha\beta}(\omega)$. Here we introduce a phenomenological conductance $G_{\rm eb}$ and write the current per unit length $j_{\rm b+e+}(x, \omega)$ from the bulk boundary b+ at $y = y_+$ to the edge channel e+ in $y > y_+$ as

$$j_{\rm b+e+}(x, \omega) = G_{\rm eb}[\phi(x, y_+, \omega) - \phi_{\rm e+}(x, \omega)], \tag{3}$$

where $\phi_{\rm e+}(x, \omega)$ is the induced potential in the edge channel e+. A similar equation holds for $j_{\rm b-e-}(x, \omega)$. The value of $G_{\rm eb}$ can

be changed over a wide range by changing the voltage of a side gate electrode placed in the vicinity of the edge channel since the distance between the edge channel and the bulk boundary can be controlled by the side-gate voltage [36, 37].

2.2. Equations for the Hall-potential distribution

Equations for $\phi(\boldsymbol{r},\omega)$ and $\phi_{\rm e\pm}(x,\omega)$ are obtained from the equation of charge conservation and written in terms of the DC conductivities, σ^0_{xx} and σ^0_{xy}, the DC susceptibility χ^0_{xx}, and the conductance $G_{\rm eb}$. The spatial dependence in $y>0$ of the diagonal component σ^0_{xx} occurs in a narrow region between y_+ and $y_{\rm b+}\equiv y_+ + \delta y$ where σ^0_{xx} decreases from the bulk value to the small value in the incompressible region. Therefore it is convenient in deriving the equations for $\phi(\boldsymbol{r},\omega)$ and $\phi_{\rm e+}(x,\omega)$ to separate a part of the 2DES in $y>0$ into the bulk region $0<y<y_+$, the boundary region $y_+<y<y_{\rm b+}$, and the incompressible region plus the edge channel $y_{\rm b+}<y<y_{\rm e+}$ (and separate a part in $y<0$ similarly). Here $y_{\rm e+}$ is the outer boundary of the edge channel e+ at which all the local conductivities vanish.

First in the bulk region ($0<y<y_+$) the equation of charge conservation becomes

$$i\omega\rho(\boldsymbol{r},\omega) = -\boldsymbol{\nabla}\cdot\boldsymbol{j}(\boldsymbol{r},\omega) = \sigma_{xx}(\omega)\boldsymbol{\nabla}^2\phi(\boldsymbol{r},\omega), \tag{4}$$

where $\rho(\boldsymbol{r},\omega)$ is the induced charge density, $\boldsymbol{\nabla}=(\nabla_x,\nabla_y)$, and $\boldsymbol{j}=(j_x,j_y)$. We assume the presence of a metallic gate above the 2DES and employ the local capacitance approximation,

$$\rho(\boldsymbol{r},\omega) = c_{\rm b}\phi(\boldsymbol{r},\omega), \tag{5}$$

where $c_{\rm b}=\varepsilon_{\rm r}\varepsilon_0/d$ is the capacitance per unit area between the bulk region of the 2DES and the metallic gate, d is the distance between these two conductors, $\varepsilon_{\rm r}$ is the relative permittivity of the semiconductor, and ε_0 is the vacuum permittivity.

Next we consider a segment of the strip ($y_{\rm b+}<y<y_{\rm e+}$) between $x-\Delta x$ and $x+\Delta x$. The equation of charge conservation in this segment is

$$i\omega Q_{\rm e+}(x,\omega) = \frac{J(x-\Delta x,\omega)-J(x+\Delta x,\omega)}{2\Delta x} + j_y^{\rm b+}(x,\omega), \tag{6}$$

where $Q_{\rm e+}(x,\omega)$ is the induced charge per unit length of the segment. The current across the line at x, $J(x,\omega)$, is given by

$$\begin{aligned} J(x,\omega) &= \int_{y_{\rm b+}}^{y_{\rm e+}} j_x(\boldsymbol{r},\omega)dy \approx \int_{y_{\rm b+}}^{y_{\rm e+}} \sigma^0_{xy}E_y(\boldsymbol{r},\omega)dy \\ &= \sigma^0_{xy}\left[\phi(x,y_{\rm b+},\omega)-\phi_{\rm e+}(x,\omega)\right], \end{aligned} \tag{7}$$

In the second equality we have used $\sigma^0_{xx}/|\sigma^0_{xy}| \ll 1$ and $\omega\chi^0_{xx}/|\sigma^0_{xy}| \approx \omega/\omega_{\rm c} \ll 1$ which is satisfied when $\omega < 10^9$ s^{-1} since $\omega_{\rm c}\sim 10^{13}$ s^{-1} for $B\sim 5$ T and the effective mass of GaAs. The current in Eq.(7) coincides with the edge current which is the summation of the induced current carried by each edge state between $y_{\rm b+}$ and $y_{\rm e+}$. [2] The current per unit length from the boundary region to the segment is

$$\begin{aligned} j_y^{\rm b+}(x,\omega) &= \sigma^0_{yx}E_x(x,y_{\rm b+},\omega) + i\omega\chi^0_{yy}E_y(x,y_{\rm b+},\omega) \\ &\quad + j_{\rm b+e+}(x,\omega). \end{aligned} \tag{8}$$

Here the current due to the transition between the edge channel and the bulk region $j_{\rm b+e+}(x,\omega)$, defined in Eq.(3), appears instead of the dissipative current in the bulk. Substituting these expressions for the currents into Eq.(6) and taking the limit of $\Delta x\to 0$ leads to

$$\begin{aligned} i\omega Q_{\rm e+}(x,\omega) &= -\sigma^0_{yx}\nabla_x\phi_{\rm e+}(x,\omega) + i\omega\chi^0_{yy}E_y(x,y_{\rm b+},\omega) \\ &\quad + j_{\rm b+e+}(x,\omega). \end{aligned} \tag{9}$$

Although the local capacitance approximation is not applicable to the edge channel with a narrow width, it is appropriate to assume that $Q_{\rm e+}(x,\omega)$ is proportional to the induced potential at the same x coordinate of the edge channel $\phi_{\rm e+}(x,\omega)$, when the length scale of the variation along x is long compared to d. Therefore we employ

$$Q_{\rm e+}(x,\omega) = C_{\rm e}\phi_{\rm e+}(x,\omega), \tag{10}$$

where $C_{\rm e}$ is the capacitance per unit length of the edge channel.

Finally we consider the charge conservation in the boundary region ($y_+<y<y_{\rm b+}$). Here we assume that the width of the boundary region δy is negligibly narrow, so that the current at $y=y_+$ from the bulk to the boundary region is equal to the current at $y=y_{\rm b+}$ from the boundary region to the edge channel. Since the difference of the current proportional to each of χ^0_{yy} and σ^0_{yx} between $y=y_+$ and $y=y_{\rm b+}$ is negligible, we obtain

$$\sigma^0_{yy}E_y(x,y_+,\omega) = j_{\rm b+e+}(x,\omega). \tag{11}$$

3. Time constants of the Hall-potential development

In the previous section we have derived the equation for the Hall potential in the bulk region as well as that in the edge channel. In this section, using these equations, we estimate time scales corresponding to the transport in the bulk region, that in the edge channel, and that between the edge channel and the bulk region.

3.1. Hall-potential development in the bulk region

Eq.(4) with Eq.(5) shows that the induced potential and the induced charge evolve according to the diffusion equation with a diffusion constant D,

$$i\omega\phi(\boldsymbol{r},\omega) = D\boldsymbol{\nabla}^2\phi(\boldsymbol{r},\omega), \quad D=\frac{\sigma^0_{xx}}{c_{\rm b}}, \tag{12}$$

since $\sigma^0_{xx}\gg\omega\chi^0_{xx}$ is satisfied as shown below. The time $\tau_{\rm b}$ necessary for the diffusion into the sample with size L becomes

$$\tau_{\rm b} = \frac{L^2}{D} = \frac{L^2c_{\rm b}}{\sigma^0_{xx}} = \frac{L^2}{\sigma^0_{xx}}\frac{\varepsilon_{\rm r}\varepsilon_0}{d}. \tag{13}$$

An estimate of $\tau_{\rm b}$ is

$$\tau_{\rm b}\sim 10^2\ {\rm s}, \tag{14}$$

[2] The edge region between $y_{\rm b+}$ and $y_{\rm e+}$ consists of the incompressible strip and the compressible one. The induced current density is larger in the incompressible strip since the diagonal resistivity is smaller there.

when we use L =1 mm, $\sigma^0_{xx} = 10^{-11}\ \Omega^{-1}$, $d = 0.1\ \mu$m, and $\varepsilon_r = 10$. At the corresponding frequency $\omega = (\tau_b)^{-1} \sim 10^{-2}\ s^{-1}$ we can neglect the imaginary part of $\sigma_{xx}(\omega)$, since

$$\frac{\omega\chi^0_{xx}}{\sigma^0_{xx}} \approx \frac{\omega}{\omega_c}\frac{2e^2/h}{\sigma^0_{xx}} \sim 10^{-8}. \tag{15}$$

3.2. Hall-potential development in the edge channel

Here we derive a time constant for the potential development in the edge channel when the edge channel is disconnected from the bulk region, that is $G_{eb} = 0$. In this case the potential response of the bulk region is absent so that $\phi(\boldsymbol{r}, \omega) = 0$. Then the equation of the time evolution in the edge channel becomes, from Eqs.(9) and (10),

$$C_e\frac{\partial\phi_{e+}}{\partial t} = -\sigma^0_{yx}\frac{\partial\phi_{e+}}{\partial x}, \tag{16}$$

and the solution is

$$\phi_{e+}(x,t) = f(x - vt), \quad v \equiv \frac{\sigma^0_{yx}}{C_e}, \tag{17}$$

where v is the group velocity of the edge magnetoplasmon and $f(x)$ is an arbitrary function. This solution reproduces that in the previous studies [38, 39]. Then the time necessary for the development of the potential at the distance L from the source contact is

$$\tau_e = \frac{C_e L}{\sigma^0_{yx}} \sim 10^{-9}\ \text{s}, \tag{18}$$

where an estimation is made by using L =1 mm and $C_e/c_b = 0.1\ \mu$m.

3.3. Hall-charge transfer from the edge to the bulk

Here we consider the development of the Hall potential in the boundary region after the potential in the edge channel is fully developed so that $\phi_{e+}(x,t)$ is independent of x and t. The corresponding time constant is the product of the resistance $1/G_{eb}$ and the effective capacitance C_{eff},

$$\tau_{eb} = \frac{C_{eff}}{G_{eb}}. \tag{19}$$

Here we assume that the Hall voltage induced across the resistance $1/G_{eb}$ is comparable to that induced in the bulk region and write $1/G_{eb} = L/\sigma^0_{yy}$. Then we obtain an estimate of τ_{eb},

$$\tau_{eb} \sim \frac{C_e L}{\sigma^0_{yy}} \sim 10^{-2}\ \text{s}, \tag{20}$$

when we use $C_{eff} = C_e$. The value of τ_{eb} varies over a wide range by changing the value of G_{eb} in terms of the side gate attached to the 2DES boundary [36, 37].

4. 1D distribution of the Hall potential

4.1. Equations for the Hall potential at low ω

In the following we focus on the slower development of the induced potential in the bulk region and calculate the potential at $\omega < 10\ s^{-1}$. At such low frequencies $\omega\chi^0_{xx}/\sigma^0_{xx} < 10^{-5}$ and therefore we neglect the $\omega\chi^0_{xx}$ term in the following calculation. Then the equations for the Hall potential in $y > 0$, Eqs.(4), (11), and (9) become

$$i\omega\phi(\boldsymbol{r},\omega) = D\boldsymbol{\nabla}^2\phi(\boldsymbol{r},\omega), \tag{21}$$

$$0 = -\sigma^0_{yy}\nabla_y\phi(x,y_+,\omega) - j_{b+e+}(x,\omega), \tag{22}$$

$$i\omega C_e\phi_{e+}(x,\omega) = -\sigma^0_{yx}\nabla_x\phi_{e+}(x,\omega) + j_{b+e+}(x,\omega), \tag{23}$$

with $j_{b+e+}(x,\omega)$ defined by Eq.(3). Since the Hall potential only changes the sign at $(x,y) \to (-x,-y)$ in the boundary condition we consider, the above set of equations is sufficient to obtain the solution.

4.2. Solution for one-dimensional distribution

First we calculate one-dimensional distribution of the Hall potential along a cross-section $x = 0$ at the center of the 2DES with length L_x. Eqs.(21), (22), and (23) can be solved for the Hall potential as a function of y by setting $x = 0$ and neglecting $\nabla^2_x\phi(x,y,\omega)$. The x component of the electric field in the edge channel, $E^e_x(\omega) \equiv -[\nabla_x\phi_{e+}(x,\omega)]_{x=0}$, is considered to be the input. The y dependence of the Hall potential in the bulk region at $x = 0$ is obtained, using Eq.(21), to be

$$\phi(0,y,\omega) = \phi(0,y_+,\omega)\frac{\sinh[K(\omega)y]}{\sinh[K(\omega)y_+]}, \tag{24}$$

where

$$K(\omega) = \frac{1+i}{\lambda(\omega)}, \quad \lambda(\omega) = \sqrt{\frac{2D}{\omega}}. \tag{25}$$

$\lambda(\omega)$ represents the penetration length [7, 9] and increases with decreasing ω. The Hall potential at the boundary $y = y_+$ is given, using Eqs.(22) and (23) with Eq.(3), by

$$\phi(0,y_+,\omega) = \frac{\sigma^0_{yx}E^e_x(\omega)L_R(\omega)}{\sigma^0_{yy}}\frac{1}{1 + i\omega C_e R(\omega)}, \tag{26}$$

where $R(\omega)$ is the series resistance between the edge channel and $y = 0$, given by

$$R(\omega) = \frac{1}{G_{eb}} + \frac{L_R(\omega)}{\sigma^0_{yy}}, \tag{27}$$

and $L_R(\omega)$ represents a length associated with the resistance of the bulk region, given by

$$L_R(\omega) = \frac{\tanh[K(\omega)y_+]}{K(\omega)}. \tag{28}$$

$L_R(\omega) = y_+ = L_y/2$ at low ω so that $\lambda(\omega) \gg L_y$, while $L_R(\omega) = K(\omega)^{-1} = \lambda(\omega)/(1+i)$ at $\lambda(\omega) \ll L_y$. The voltage between the edge channel and the bulk boundary, on the other hand, is

$$\phi_{e+}(0,\omega) - \phi(0,y_+,\omega) = \frac{\sigma^0_{yx}E^e_x(\omega)}{G_{eb}}\frac{1}{1 + i\omega C_e R(\omega)}. \tag{29}$$

This shows that the potential jump is proportional to $1/G_{\rm eb}$, while Eq.(26) shows that the voltage across the bulk ($0 < y < y_+$) is proportional to $L_R(\omega)/\sigma^0_{yy}$.

Fig. 1 demonstrates the y dependence of the Hall potential at $x = 0$ for three different values of ω. Since the Hall potential is normalized by $\phi_0 = \sigma^0_{yx}E^{\rm e}_x(\omega)(L_y/2)(\sigma^0_{yy})^{-1}$, it is determined by values of y/L_y, $\omega L_y^2/D$, $\sigma^0_{yy}/(G_{\rm eb}L_y)$, and $C_{\rm e}/(c_{\rm b}L_y)$. The Hall potential in the bulk region $\phi(0, y, \omega)$ has a uniform gradient at $\omega\tau_y \ll 1$ where $\tau_y = L_y^2/D$ is the time constant for the diffusion into the sample. At $\omega\tau_y \gg 1$, on the other hand, the penetration length $\lambda(\omega)$ of the potential $\phi(0, y, \omega)$ becomes much shorter than the sample width L_y and at the same time the potential $\phi(0, y, \omega)$ oscillates as a function of y [9]. The jump in the Hall potential appears between the bulk boundary and the edge channel [Eq.(29)], which is proportional to $1/G_{\rm eb}$. The presence of the imaginary part of the Hall potential shown in Fig. 1(b) indicates a delay in the response to the input $E^{\rm e}_x(\omega)$. The delay in the bulk region becomes substantial at large $\omega\tau_y$. However, it is negligible in the voltage between the bulk boundary and the edge channel, because $|\omega C_{\rm e}R(\omega)| < 10^{-2}$ in the frequency range shown in Fig. 1.

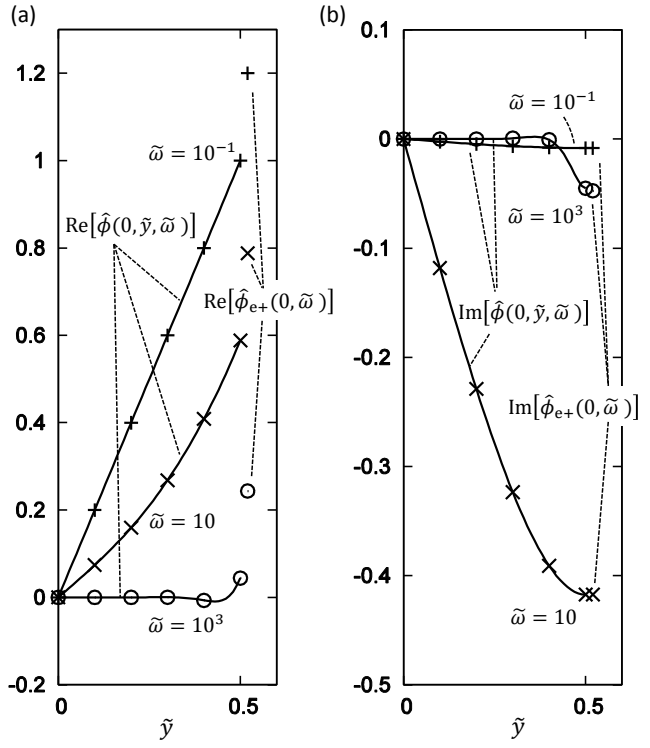

Figure 1: (a) The real part and (b) the imaginary part of the Hall potential are plotted as a function of y (in the direction perpendicular to the edge channel) at the center of the 2DES $x = 0$ for three values of the angular frequency ω of the AC source-drain voltage. $\phi(0, y, \omega)$ and $\phi_{\rm e+}(0, \omega)$ denote the induced potential in the bulk and that in the edge channel, respectively. Variables are normalized as $\hat{\phi} \equiv \phi/\phi_0$ and $\hat{\phi}_{\rm e+} \equiv \phi_{\rm e+}/\phi_0$ with $\phi_0 = \sigma^0_{yx}E^{\rm e}_x(\omega)(L_y/2)(\sigma^0_{yy})^{-1}$, $\tilde{y} \equiv y/L_y$, and $\tilde{\omega} \equiv \omega L_y^2/D$. Values used are $\tilde{\omega} = 10^{-1}(+), 10(\times), 10^3(\bigcirc)$, $\sigma^0_{yy}/(G_{\rm eb}L_y) = 0.1$, and $C_{\rm e}/(c_{\rm b}L_y) = 10^{-4}$.

4.3. Crossover between edge and bulk transports

The current through the 2DES at $x = 0$ in $y > 0$ can be divided into that through the bulk region ($0 < y < y_{\rm b+}$) $J_{\rm b}$ and that through the edge region ($y_{\rm b+} < y < y_{\rm e+}$) $J_{\rm e}$. Each of $J_{\rm b}$ and $J_{\rm e}$ is the Hall current, if we exclude a negligible contribution from the diffusion current, and is proportional to the Hall voltage in each region, which in turn is proportional to the resistance for the current along y, given by each term of Eq.(27). Therefore the current ratio reduces to

$$\frac{J_{\rm e}}{J_{\rm b}} = \frac{\phi_{\rm e+}(0,\omega) - \phi(0, y_+, \omega)}{\phi(0, y_+, \omega)} = \frac{1/G_{\rm eb}}{L_R(\omega)/\sigma^0_{yy}}. \tag{30}$$

When $\omega = 0$ and $L_y/(2\sigma^0_{yy}) > 1/G_{\rm eb}$, the bulk current is dominant over the edge current. By increasing $1/G_{\rm eb}$, for example by the side-gate voltage, the edge current can be made larger than the bulk current and a crossover occurs from the bulk transport to the edge transport. In the case of $\omega \neq 0$, we find from Eq.(30) that the crossover is possible even at a fixed $1/G_{\rm eb}$ by increasing ω, since the decreased penetration length $\lambda(\omega)$ reduces the bulk current.

5. 2D distribution of the Hall potential

5.1. Boundary condition at current contacts

We now study the two-dimensional distribution of the induced potential in the 2DES which is connected to the source electrode at $x = x_- \equiv -L_x/2$ and the drain electrode at $x = x_+ \equiv L_x/2$. Potentials of source and drain electrodes are $\phi_{\rm s}e^{i\omega t}$ and $-\phi_{\rm s}e^{i\omega t}$, respectively. Therefore the boundary condition for the Hall potential is

$$\phi(x_-, y, \omega) = \phi_{\rm s}, \;\; \phi(x_+, y, \omega) = -\phi_{\rm s}, \tag{31}$$

$$\phi_{\rm e+}(x_-, \omega) = \phi_{\rm s}, \;\; \phi_{\rm e+}(x_+, \omega) = -\phi_{\rm s}. \tag{32}$$

Under such a boundary condition, the Hall potential changes the sign when (x, y) is changed to $(-x, -y)$. In the following we calculate the normalized Hall potential, $\phi(x, y, \omega)/\phi_{\rm s}$ and $\phi_{\rm e+}(x, \omega)/\phi_{\rm s}$, which is determined by giving values of x/L_x, y/L_y, L_x/L_y, $\omega\tau_y$, $\sigma^0_{yy}/(G_{\rm eb}L_y)$, $\sigma^0_{yx}/\sigma^0_{yy}$, and $C_{\rm e}/(c_{\rm b}L_y)$.

5.2. Discretized coordinates

In calculating numerically the two-dimensional distribution of the Hall potential, we introduce the following sampling points,

$$x_n = x_- + n\Delta x \; (n = 0, 1, \cdots, N), \;\; \Delta x = L_x/N, \tag{33}$$

$$y_m = y_- + m\Delta y \; (m = 0, 1, \cdots, M), \;\; \Delta y = L_y/M, \tag{34}$$

The derivatives with respect to x appearing Eqs.(21) and (23) become, with $\phi_{n,m} = \phi(x_n, y_m, \omega)$ and $\phi^{\rm e+}_n = \phi_{\rm e+}(x_n, \omega)$,

$$\nabla_x\phi_{\rm e+}(x_n, \omega) = (\phi^{\rm e+}_{n+1} - \phi^{\rm e+}_{n-1})/(2\Delta x), \tag{35}$$

$$\nabla^2_x\phi(x_n, y_m, \omega) = (\phi_{n+1,m} - 2\phi_{n,m} + \phi_{n-1,m})/\Delta x^2. \tag{36}$$

The derivatives with respect to y are similarly calculated. There are two exceptions, however. The first exception is the derivative at $y = y_+$ ($m = M$) where we use

$$\nabla_y\phi(x_n, y_m, \omega) = (\phi_{n,m} - \phi_{n,m-1})/\Delta y, \tag{37}$$

because the variable $\phi_{n,M+1}$ is absent. The second exception is the derivative of $\phi_{e+}(x,\omega)$ at $x = x_+ - \Delta x$ ($n = N-1$) where we use

$$\nabla_x \phi_{e+}(x_n,\omega) = (\phi_n^{e+} - \phi_{n-1}^{e+})/\Delta x, \tag{38}$$

due to the discontinuity of $\phi_{e+}(x_n,\omega)$ between $n = N-1$ and N, which is visible in the results presented below. [3]

5.3. Results

Fig. 2 represents calculated two-dimensional distributions of the Hall potential for $\omega = 0$. The DC Hall-potential distribution in Fig. 2(a) shows a concentration of the electric field at two corners, $(x,y) = (x_-, y_-)$ and (x_+, y_+), as in the calculation of the bulk 2DES [40]. When $\sigma_{yy}^0/(G_{eb}L_y)$ is increased [Fig. 2(b)], the potential jump between the edge channel and the bulk boundary becomes significant and the concentration of the electric field at the corners is relaxed.

Fig. 3 shows the two-dimensional distribution for the AC source-drain voltage with $\omega\tau_y = 10^3$. The induced potential penetrates from the edge channel to the bulk region as is already shown in the one-dimensional distribution [Fig. 1]. Fig. 4 demonstrates that the y dependence of the numerically-calculated Hall potential along the cross-section at $x = 0$ agrees well with the analytical solution for the one-dimensional distribution. The difference is at most 20% in both $\sigma_{yy}^0/(G_{eb}L_y) = 10^{-3}$ [Fig. 4(a)] and $\sigma_{yy}^0/(G_{eb}L_y) = 0.1$ [Fig. 4(b)], which is due to the error caused by replacing the differential with the difference, since deviations between the numerical and analytical solutions decrease with increasing $N(= M)$.

The two-dimensional distribution shows an additional penetration from each of the source and drain contacts. Such a penetration can also be derived analytically from Eq.(21) by setting $y = 0$ and neglecting $\nabla_y^2\phi(x,y,\omega)$. The Hall potential along the line $y = 0$ is obtained to be

$$\phi(x,0,\omega) = -\phi_s \frac{\sinh[K(\omega)x]}{\sinh[K(\omega)x_+]}, \tag{39}$$

for the boundary condition given in Eq.(31), and shows the same spatial variation as the penetration from the edge channel, given in Eq.(24).

6. Conclusions

We have developed a theoretical formulation which is able to determine the AC transport in both the bulk region and the edge channel, when a quantum Hall system is driven by the AC source-drain voltage. At high frequencies, the Hall potential develops through the edge channel in terms of the propagation of the edge magnetoplasmon with velocity proportional to the DC Hall conductivity σ_{yx}^0. When the frequency is lowered, the induced Hall charge in the edge channel tunnels to the bulk boundary and subsequently diffuses into the inside of the bulk region with the diffusion constant proportional to the DC diagonal conductivity σ_{xx}^0. The time constant for the diffusion in the bulk region is many orders of magnitude longer than that for the propagation in the edge channel because of the large ratio of $\sigma_{yx}^0/\sigma_{xx}^0$ apart from the width difference. We have found from calculated two-dimensional distributions of the Hall potential that the penetration of the Hall potential also occurs from each of the source and drain contacts, in addition to that from the edge channel.

[3] The discontinuity is due to the absence of the second derivative $\nabla_x^2\phi_{e+}(x,\omega)$ in Eq.(23). The boundary condition at $x = x_-$ and Eq.(23) determines $\phi_{e+}(x,\omega)$ from $x = x_-$ to $x = x_+ - \Delta x$ in which the boundary condition at $x = x_+$ is not used.

References

[1] K. von Klitzing, G. Dorda, M. Pepper, Phys. Rev. Lett. 45 (1980) 494.
[2] S. Kawaji, J. Wakabayashi, in *Physics in High Magnetic Fields*, edited by S. Chikazumi, N. Miura (Springer, Berlin, 1981) p. 284.
[3] D. C. Tsui, H. L. Stormer, A. C. Gossard, Phys. Rev. Lett. 48 (1982) 1559.
[4] M. Pepper, J. Wakabayashi, J. Phys. C 16 (1983) L113.
[5] Y. Iwasa, G. Kido, N. Miura, Solid State Commun. 46 (1983) 239.
[6] B. B. Goldberg, T. P. Smith, M. Heiblum, P. J. Stiles, Surf. Sci. 170 (1986) 180.
[7] I.M. Grodnensky, D. Heitmann, K. von Klitzing, A.Y. Kamaev, Phys. Rev. B 44 (1991) 1946.
[8] I.M. Grodnensky, D. Heitmann, K. von Klitzing, A.Y. Kamaev, in *High Magnetic Fields in Semiconductor Physics*, edited by G. Landwehr (Springer, Berlin, 1992) p. 135.
[9] H. Akera, Physica E 43 (2011) 1240.
[10] J. Weis, Y.Y. Wei, K. v. Klitzing, Physica B 256-258 (1998) 1.
[11] N. G. Kalugin, B. E. Sağol, A. Buss, A. Hirsch, C. Stellmach, G. Hein, G. Nachtwei, Phys. Rev. B 68 (2003) 125313.
[12] A. Buss, F. Hohls, F. Schulze-Wischeler, C. Stellmach, G. Hein, R. J. Haug, G. Nachtwei, Phys. Rev. B 71 (2005) 195319.
[13] T.J. Kershaw, A. Usher, A.S. Sachrajda, J. Gupta, Z.R. Wasilewski, M. Elliott, D.A. Ritchie, M.Y. Simmons, New Journal of Physics 9 (2007) 71.
[14] H. Akera, J. Phys. Soc. Jpn. 78 (2009) 023708.
[15] B. J. van Wees, E. M. M. Willems, C. J. P. M. Harmans, C. W. J. Beenakker, H. van Houten, J. G. Williamson, C. T. Foxon, J. J. Harris, Phys. Rev. Lett. 62 (1989) 1181.
[16] S. Komiyama, H. Hirai, S. Sasa, S. Hiyamizu, Phys. Rev. B 40 (1989) 12566.
[17] B. J. van Wees, E. M. M. Willems, L. P. Kouwenhoven, C. J. P. M. Harmans, J. G. Williamson, C. T. Foxon, J. J. Harris, Phys. Rev. B 39 (1989) 8066.
[18] R. J. Haug, K. von Klitzing, Europhys. Lett. 10 (1989) 489.
[19] P. L. McEuen, A. Szafer, C. A. Richter, B. W. Alphenaar, J. K. Jain, A. D. Stone, R. G. Wheeler, R. N. Sacks, Phys. Rev. Lett. 64 (1990) 2062.
[20] S. Komiyama, H. Nii, M. Ohsawa, S. Fukatsu, Y. Shiraki, R. Itoh, H. Toyoshima, Solid State Commun. 80 (1991) 157.
[21] K. Ikushima, H. Sakuma, S. Komiyama, K. Hirakawa, Phys. Rev. Lett. 93 (2004) 146804.
[22] D. B. Mast, A. J. Dahm, A. L. Fetter, Phys. Rev. Lett. 54 (1985) 1706.
[23] D. C. Glattli, E. Y. Andrei, G. Deville, J. Poitrenaud, F. I. B. Williams, Phys. Rev. Lett. 54 (1985) 1710.
[24] R. C. Ashoori, H. L. Stormer, L. N. Pfeiffer, K. W. Baldwin, and K. West, Phys. Rev. B 45 (1992) 3894.
[25] V. I. Talyanskii, A. V. Polisski, D. D. Arnone, M. Pepper, C. G. Smith, D. A. Ritchie, J. E. Frost, G. A. C. Jones, Phys. Rev. B 46 (1992) 12427.
[26] G. Ernst, R. J. Haug, J. Kuhl, K. von Klitzing, K. Eberl, Phys. Rev. Lett. 77 (1996) 4245.
[27] A. L. Fetter, Phys. Rev. B 32 (1985) 7676.
[28] V. A. Volkov, S. A. Mikhailov, JETP Lett. 42 (1985) 556.
[29] V. A. Volkov, S. A. Mikhailov, Sov. Phys. JETP 67 (1988) 1639.
[30] I. L. Aleiner, L. I. Glazman, Phys. Rev. Lett. 72 (1994) 2935.
[31] N. B. Zhitenev, R. J. Haug, K. v. Klitzing, K. Eberl, Phys. Rev. Lett. 71 (1993) 2292.
[32] N. B. Zhitenev, R. J. Haug, K. v. Klitzing, K. Eberl, Phys. Rev. B 49 (1994) 7809.

[33] M. D. Johnson, G. Vignale, Phys. Rev. B 67 (2003) 205332.
[34] H. Kamata, T. Ota, K. Muraki, T. Fujisawa, Phys. Rev. B 81 (2010) 085329.
[35] N. Kumada, H. Kamata, T. Fujisawa, Phys. Rev. B 84 (2011) 045314.
[36] I. A. Larkin, J. H. Davies, Phys. Rev. B 52 (1995) R5535.
[37] K. Oto, S. Takaoka, K. Murase, Physica B 298 (2001) 18.
[38] N. B. Zhitenev, R. J. Haug, K. v. Klitzing, K. Eberl, Phys. Rev. B 52 (1995) 11277.
[39] M. Hashisaka, H. Kamata, N. Kumada, K.Washio, R. Murata, K. Muraki, T. Fujisawa, Phys. Rev. B 88 (2013) 235409.
[40] J. Wakabayashi, S. Kawaji, J. Phys. Soc. Jpn. 44 (1978) 1839.
[41] W. Chen, T. P. Smith, M. Büttiker, M. Shayegan, Phys. Rev. Lett. 73 (1994) 146.
[42] T. Christen, M. Büttiker, Phys. Rev. B 53 (1996) 2064.

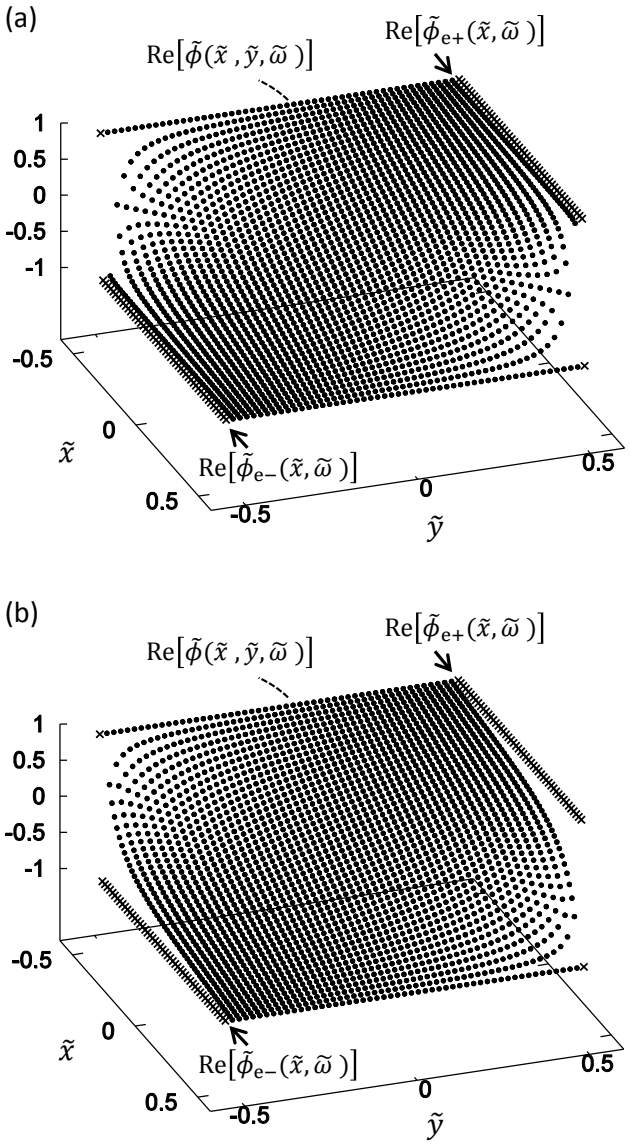

Figure 2: The real part of the DC Hall potential ($\omega = 0$) is plotted as a function of x and y [the source (drain) contacts are in the negative (positive) x side]. $\phi(x, y, \omega)$ (•) and $\phi_{e\pm}(x, \omega)$ (×) denote the induced potential in the bulk and that in the edge channel, respectively. The upper figure (a) [lower figure (b)] shows the Hall-potential distribution in a smaller [larger] effective resistance G_{eb}^{-1} between the edge channel and the bulk boundary of (a) $\sigma_{yy}^0/(G_{eb}L_y) = 10^{-3}$ [(b) $\sigma_{yy}^0/(G_{eb}L_y) = 0.1$], in which the Hall potential at the bulk boundary (•) is close to [deviated from] that in the edge channel (×). Variables are normalized as $\tilde{\phi} \equiv \phi/\phi_s$ and $\tilde{\phi}_{e\pm} \equiv \phi_{e\pm}/\phi_s$ with ϕ_s the potential at the source contact, $\tilde{x} \equiv x/L_x$, and $\tilde{y} \equiv y/L_y$. Other values used are $\sigma_{yx}^0/\sigma_{yy}^0 = 10^7$, $C_e/(c_b L_y) = 10^{-4}$, $L_x/L_y = 1$, and $N = M = 50$.

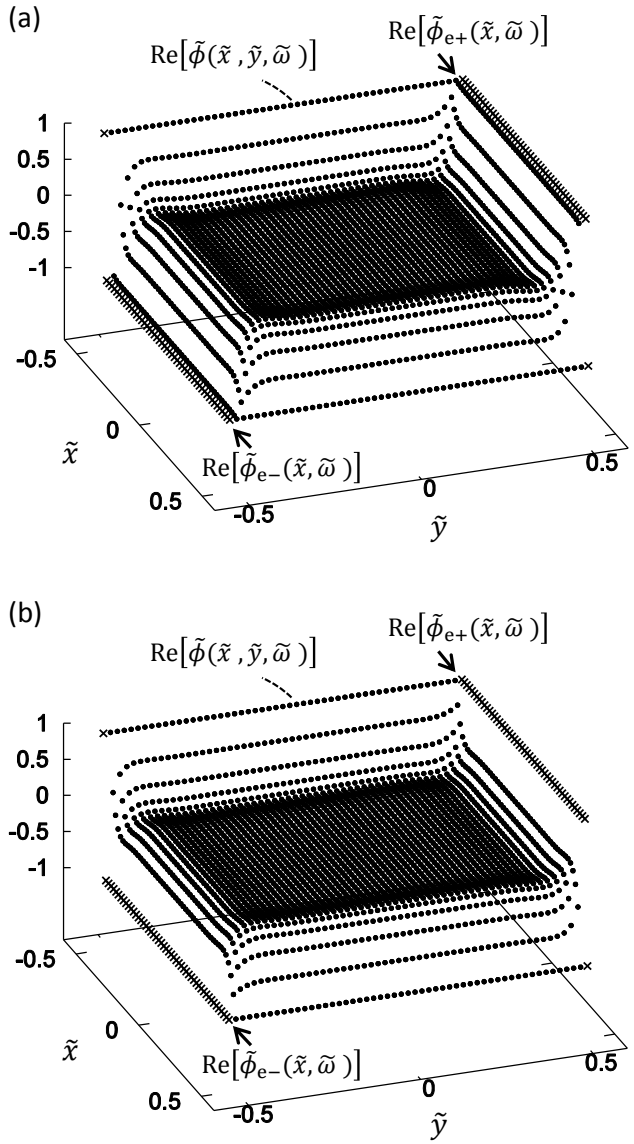

Figure 3: The real part of the AC Hall potential when $\tilde{\omega} = \omega\tau_y = \omega L_y^2/D = 10^3$ for (a) $\sigma^0_{yy}/(G_{\mathrm{eb}}L_y) = 10^{-3}$ and (b) $\sigma^0_{yy}/(G_{\mathrm{eb}}L_y) = 0.1$. Values of other parameters are the same as in Fig. 2. See the caption of Fig. 2 for more description.

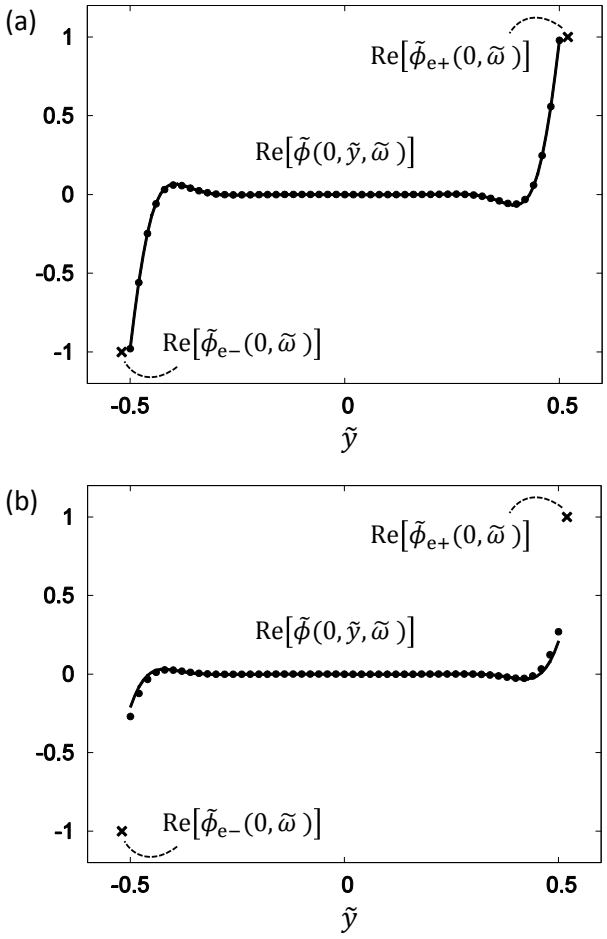

Figure 4: The comparison of the real part of the AC Hall potential at $x = 0$ between the numerical two-dimensional (2D) calculation ($\bullet$ and $\times$) and the analytical one-dimensional (1D) solution (solid line and $\times$) when $\tilde{\omega} = \omega L_y^2/D = 10^3$ for (a) $\sigma^0_{yy}/(G_{\mathrm{eb}}L_y) = 10^{-3}$ and (b) $\sigma^0_{yy}/(G_{\mathrm{eb}}L_y) = 0.1$. The 1D solution in this figure is normalized by multiplying $\mathrm{Re}[\tilde{\phi}_{e+}(2D)]/\mathrm{Re}[\hat{\phi}_{e+}(1D)]$ so that the value at the edge channel coincides with that of the 2D calculation. Values of other parameters are the same as in Fig. 2.